Cornell University
Space Systems Design Studio
Electrolysis Propulsion Research Project

Cornell University

Lunar CubeSat Project

End of Semester Report
Steven Dourmashkin (sjd227)
Spring 2014

Subsystem: ADCNS

May 20th, 2014

Table of Contents

1. Abstract 2

2. Introduction 2

3. Design 3

   3.1. Cold Gas Micro-Thruster 3

   3.2. Propellant 4

   3.3. Regulator 7

   3.4. Tank Size 8

   3.5. Isolation Valve 9

   3.6. CMOS Image Processing 10

   3.7. CMOS Hardware 12

4. Analysis 14

5. Results 17

6. Future Work 19

7. Conclusion 21

8. References 21

   8.1. Cold Gas Thrusters 21

   8.2. R-134a Propellant 22

   8.3. MEMS Isolation Valve 22

   8.4. CMOS Image Sensor 22

   8.5. General 23

9. Appendix 23

1. Abstract

This report describes the design and analysis of the Attitude Control System (ACS) cold gas thruster (CGT) system and complementary metal-oxide-semiconductor (CMOS) attitude determination sensors for the Cornell Lunar CubeSat Project. Trade studies involved in the selection of the Moog 58-149 cold gas micro-thruster for the CGT system are presented. Then, the pros and cons of several propellant candidates that ultimately lead to the selection of carbon dioxide are stated. The regulator, which is required to reduce the cold gas pressure to the operation conditions of the micro-thruster, is described, followed by the storage tank, which must enable ±5° of pointing precision and at least 360 degrees of reorientation, and must fit within the constrained space of the spacecraft. The isolation valve, which would reduce propellant leakage in the months prior to launch and may be required to allow the pressurized vessel onboard the SLS/Orion EM-1, is also discussed. Because the addition of the isolation valve adds much complexity to the system without clear benefits, it has been currently omitted from the design, yet should be incorporated in the future model. After the CGT system is described, the use of CMOS image sensors for full attitude determination, as well as the required hardware, is explained. Finally, the testing procedures for the CGT system and CMOS sensors, as well as future improvements for both components, are discussed.

2. Introduction

The Cornell Lunar CubeSat Project involves the design of a 6U satellite to be entered into the NASA Centennial Challenge, with a primary goal of being the first satellite to achieve a verifiable lunar orbit, determined by a prescribed minimum number of lunar orbital periods. Upon separation from the SLS/Orion EM-1, the 6U satellite will perform a spin-up maneuver to achieve a stable spin, after which it will separate into two 3U-sized satellites that will utilize water electrolysis for propulsion. In order to collect hydrogen and oxygen gas during electrolysis, the spin-rate of the satellite is fairly high: 6 rad/s, or approximately 1 rotation per second. While this high spin-rate creates a very stable spin about each satellite's major axis of inertia, the resulting large angular momentum makes reorientation difficult. Since reactions wheels cannot be used effectively on the spinning spacecraft, cold gas thrusters were decided to be the most appropriate attitude actuator due to their simplicity and the relatively short mission lifetime of the spacecraft (making leakage concerns less significant). The role of the ADCNS Subsystem on the Lunar CubeSat team was to design and analyze the effectiveness of a cold gas thruster system, which must execute the initial spin-up maneuver, provide a total reorientation of at least 360° throughout the mission lifetime, and point the spacecraft's z-axis to within a precision of ±5°[1]. Carbon dioxide (CO_2) propellant was chosen as the most suitable propellant primarily because it is (a) readily available in small disposable cylinders as a commercial off-the-shelf (COTS) product; (b) a liquid with a high vapor pressure within the expected operation temperatures of the satellite, enabling greater storage in a given tank without the use of heaters; and (c) a commonly used propellant in other cold gas thruster systems.

[1] LCP-ADCNS-002: ADCNS Requirements

In addition, the ADCNS subsystem was in charge of determining the hardware required for full attitude determination, which is limited due to the spacecraft's small size, high spin rate, and lunar trajectory. The most effective solution was found to be using three CMOS image sensors to identify the Earth, Moon, and Sun in order to reference the spacecraft's body frame to the Earth-Centered Inertial (ECI) frame. In addition, the CMOS sensors will also be used as a second estimator of the spacecraft's angular rate by analyzing image blur. The development of the CGT system and CMOS attitude determination sensors will be described in their entirety throughout the rest of this report.

3. Design

3.1. Cold Gas Micro-Thruster

The cold gas micro-thruster consists of simply a solenoid valve that, when commanded open, expels gas through its nozzle. Each "3U" satellite will have one cold gas micro-thruster, placed a maximal distance from the spacecraft's center of mass in order to maximize torque, that will be fired at least once per spin period during a reorientation maneuver.

The selection of a cold gas micro-thruster was first limited to several objectives and constraints. First, size and mass were minimized; a mass of approximately 50 g was deemed an appropriate maximum. Next, the valve's combined open/close response time was decided to be at most 50 milliseconds, which, given a spin rate of 6 rad/s, causes each pulse to span 17.2 degrees of the spacecraft's rotation. Since the direction of the applied torque changes with the satellite's rotation, the effective torque in tilting the satellite decreases as the pulse time increases. For a pulse time of 50 ms, the effective torque is essentially 99.63% of the original torque, as calculated by the following equation:

$$\tau_{eff} = \tau \cdot 2\sin\left(\frac{\omega_{SC}\Delta t_{pulse}}{2}\right) \Big/ \omega_{SC}\Delta t_{pulse} \qquad \textbf{(Eq. 1)}$$

where τ is the torque applied by the micro-thruster, ω_{SC} is the spacecraft's spin-rate, and Δt_{pulse} is the pulse time.

In addition, the thruster must provide at least 0.12 Nm of thrust, which, given carbon dioxide as the propellant at 25°C, would require approximately 5677 pulses, or 94.6 minutes at 1 Hz pulsing (i.e., pulsing once per revolution), to reach a total reorientation of 360°. Thus, a thrust of 0.12 N would ensure that the total number of pulses remains under the expected maximum of most micro-thrusters. Further, the maximum thrust was determined to be 15.75 Nm, which, when the main propulsion tank is empty, would yield a reorientation of 10° per pulse—or, in other words, a precision of ±5°—using Carbon Dioxide as the propellant. Next, the operating voltage and power consumption were aimed to be between 5 and 12 V_{DC} and under 10 W. Finally, the selection of a cold gas micro-thruster was limited by the manufacture's availability, as 4 units are needed: two flight and two engineering units.

Based on these objectives and constraints, possible cold gas micro-thrusters for the CGT system were narrowed down to eight candidates, as provided in Table 1. As highlighted in the table, the Moog 58-149 was ultimately chosen due to its relatively high

thrust and, in particular, its availability, as claimed by Moog employee Richard Meinhold. Although the selected CGT regulator has an outlet pressure of 87 psi, which is directly within the operating range of the Moog 58-112 thruster, this thruster has been out of production since the 1980s; therefore, purchasing the thruster would be difficult, costly, and unnecessary since the Moog 58-149 can still operate at lower pressures, but will have a lower thrust that is proportional to the supplied gas pressure. Additionally, the Marotta Cold Gas Micro-Thruster would be an excellent option for the CGT system, especially since it can handle pressures of up to 2240 psi (thus not requiring a regulator), but it was eventually omitted due to its large envelope size of 58.42 mm x 22.10 mm. To meet the power operating voltage and valve power requirements of the Moog 58-149 thruster, which are above the capabilities of the satellite's batteries, an additional capacitor network will be used. Additional details of the Moog 58-149 thruster are provided in Appendix A.

Table 1: Candidate Cold Gas Micro-Thrusters

Manufacturer	Moog	Moog	Moog	Moog	Moog	Marotta
Model	58-102/103/113	58-112	58-142	58-149	58-151	Cold Gas Micro-Thruster
Thrust [Nm]	1.11/5.55/3.33	1.11	0.12	3.56	0.12	0.05 (100 psi), 0.526 (500 psi), 2.360 (2400 psi)
ISP [s]	68	68	>57	65	65	65
Cycle Life [cycles]	10,000	10,000	20,000	20,000	1,000,000	-
Engine Mass [g]	15	15	16	22.7	70	<60
Response (Open) [ms]	3.5	3.5	3.5	3.5	5	<5
Response (Close) [ms]	3.5	3.5	3.5	3.5	3	<5
Operating Pressure [psi]	90 – 125	70 - 110	50-300	215	0-400	100-2240
Operating Voltage [V]	24-32	24-32	-	28	-	2.5
Valve Power (Open) [W]	30	30	<35	30	10.5	<1
Envelope Size [mm]	24.7 x 14.5	24.7 x 14.5	20.3x14	25.4 x 15.24	40.87x19.05	58.42x22.10

*NOTE: ISP determined using nitrogen gas at operating conditions

3.2. Propellant

A major constraint for propellant selection was the limited space available onboard each "3U" CubeSat. To maximize reorientation for gas propellants, ISP and molar mass should be maximized, as illustrated by the following equation:

$$\Delta\phi_{tot} = \frac{rI_{tot}}{H} = \frac{r\left(ISP \cdot g_0 m_0\right)}{H} = \frac{r\left[ISP \cdot g_0\left(\frac{PV}{RT}MM\right)\right]}{H} = \frac{rg_0 PV}{HRT}\left(ISP \cdot MM\right) \quad \textbf{(Eq. 2)}$$

where r is the thruster's distance away from the spacecraft's center of mass, I_{tot} is the total impulse provided by the thruster, H is the spacecraft's angular momentum, g_0 is standard gravity, m_0 is the initial mass of the propellant, V is the volume of the propellant storage tank, R is the ideal gas constant, and P, T, and MM are the pressure, temperature, and molar mass of the propellant. Values of molar mass and ISP for several cold gas propellants are provided in Table 2: Cold Gas Thruster Propellants.

Although Hydrogen and Helium both have a very high ISP, they were immediately eliminated due to their low molar mass. Nitrogen was a strong candidate since it is the most frequently used cold gas propellant[2]; has a moderately high ISP and molecular weight, and a lack of contamination concerns; and is commonly sold in small, disposable gas cartridges, which is required for our mission due to limited available space for the CGT system. However, using the largest tank size that fits the current "3U" design—a Leland 98 mL disposable cartridge —the spin rate would have to be reduced to 5.2 rad/s to allow 360° of reorientation using Nitrogen gas at the maximum fill pressure of the Leland cylinders: 2750 psi. Therefore, propellants with a higher molar mass and ISP product were investigated. R-134a was found to have the highest molar mass / ISP product of all cold gas propellants; further, R-134a has been used in other CubeSat cold gas thruster systems, including projects from the Missouri University of Science and Technology, the University of Missouri-Rolla, University of Texas, and Washington University[3]. Unfortunately, a COTS disposable gas cartridge prefilled with R-134a does not exist. Thus, the cold gas propellant with the highest molar mass / ISP product sold in a disposable gas cartridge was selected as a candidate for the cold gas propellant of the CGT system: Argon (Ar), sold by Leland Gas Technologies.

In addition, carbon dioxide was chosen as a second candidate for several key reasons. At the average operating temperature of the satellite (approximated as 25°C for analysis), carbon dioxide has a vapor pressure of 838.8 psi, as provided in Figure 1. Thus, shown in Figure 2, carbon dioxide behaves as a liquid at this temperature. As the gaseous carbon dioxide is used as propellant, the liquid quickly evaporates to replenish it, keeping the pressure inside the propellant tank constant until all the liquid evaporates[4]. The fact that carbon dioxide behaves partially as a liquid allows much more propellant to be stored within a given storage tank than pure gas; for instance, a 35 mL Leland cartridge containing 24 grams of carbon dioxide can only hold approximately 6 g of Nitrogen at 2750 psi. Therefore, carbon dioxide reduces the size of the propellant storage tank. Second, the vapor pressure of carbon dioxide remains greater than the operating pressure of the Moog 58-149 thruster, 215 psi, above approximately -27°C. This ensures that, with the use of a regulator at normal satellite temperatures, the thruster can operate properly and maximum thrust can theoretically be achieved.

---

[2] Anis, Assad (2012). "Cold Gas Propulsion System – An Ideal Choice for Remote Sensing Small Satellites". *NED University of Engineering and Technology*. Web. 07 Mar. 2014.

[3] Seubert, Carl R., Miller, Shawn W., Siebert, Joseph R. , Stweart, Abbie M., Pernicka, Henry J. "Feasibility of Developing a Refrigerant-Based Propulsion System for Small Spacecraft". *University of Missouri-Rolla*. 04 March. 2007. Web. 12 Apr. 2014.

[4] Berkovitz, D. S., "System Characterization and Online Mass Property Identification of the SPHERES Formation Flight Testbed," S.M. Thesis, Department of Aeronautics and Astronautics, Massachusetts Institute of Technology, Cambridge, MA, 2008.

Table 2: Cold Gas Thruster Propellants

Propellant	Molar Mass [g/mol]	ISP [s]
Hydrogen	2.0	272
Helium	4.0	165
Nitrogen	28.0	65
Dinitrogen monoxide	44.0	67
Argon	40.0	50
Krypton	83.8	37
Xenon	131.3	28
Freon 12	121.0	37
Freon 14	88.0	49
R-134a	102.03	49
R-123	152.93	32
Ammonia (liquid)	17.0	96
Carbon Dioxide (liquid)	44.0	61
Sulfur Hexafluoride (liquid)	146.1	42

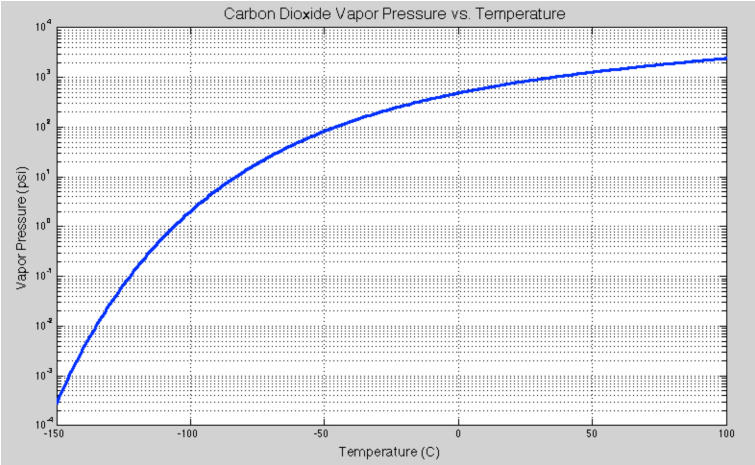

Figure 1: Vapor Pressure of Carbon Dioxide

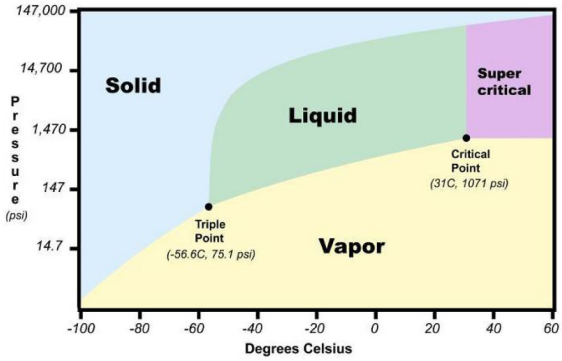

Figure 2: Phase Diagram of Carbon Dioxide

Another liquefiable gas that could theoretically be suitable for the CGT system is ammonia, which has a much lower vapor pressure than carbon dioxide, as illustrated in Figure 3. By using ammonia, the Moog 58-149 micro-thruster could potentially be used

without a regulator, since, below 60°C, the vapor pressure of ammonia remains below 385, which, as specified by Moog employee Richard Meinhold, is the stall pressure of the thruster (i.e., the pressure at which the thruster valve cannot open). Using ammonia, then, assumes that the spacecraft does not generally exceed 60°C during its lunar trajectory. Because Leland Gas Technologies does not provide appropriate disposable cartridges prefilled with Ammonia or a liquefiable gas of similar vapor pressure characteristics (such as SF_6), ammonia was not considered a candidate propellant, yet an ammonia-based CGT system should be analyzed for future consideration, since a CGT system without a regular may be preferable due to reduced size and leakage.

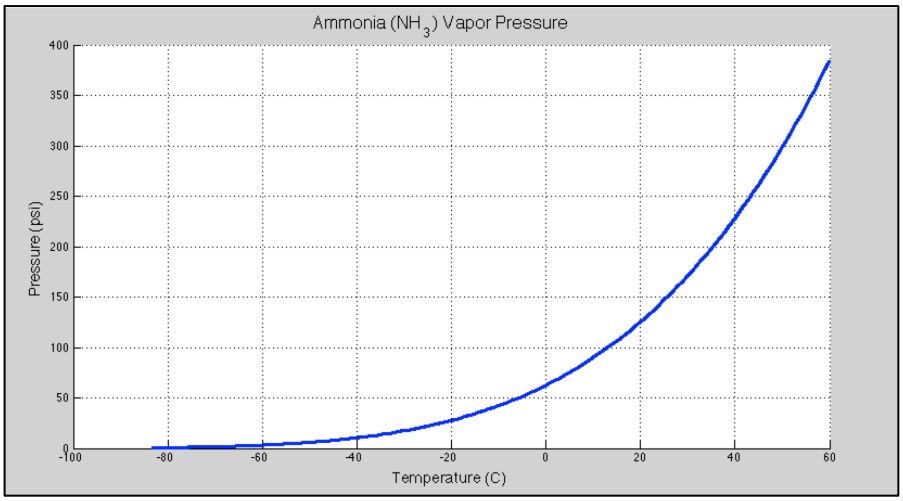

Figure 3: Vapor Pressure of Ammonia (NH_3)

3.3. Regulator

In order to reduce the pressure of the propellant to the operating pressure (215 psi) and, more importantly, below the stall pressure (325 psi) of the Moog 58-149 cold gas micro-thruster, a regulator is required. Limited by size and mass, several candidate regulators that can support argon or carbon dioxide are provided below in Table 3. Since the propellant tank is limited to disposable gas cartridges, the regulator selection was narrowed down to the two Leland regulators, since they contain a built-in puncture device; if another regulator were to be chosen, a separate puncture device would need to be installed into the CGT system, which, as illustrated in Figure 4, is relatively large: approximately 1.5 m in length and 1 m in diameter. Although the Leland NR-18 can support a higher outlet pressure, allowing potentially greater thruster efficiency, it is significantly larger than the NR-10 regulator, and is not in-line, in turn complicating the design. Therefore, the Leland NR-10 regulator was selected for use in the CGT system.

Table 3: Regulators for the CGT System

Manufacturer	Item Name	Max. Inlet Pressure [psi]	Min Outlet Pressure [psi]	Max Outlet Pressure [psi]	Size (length, diam.) [in]	Mass [g]
Leland	NR-18	3000	14.5	110	2.65 x 0.9	230
Leland	NR-10	3000	30	87	2.476 x 0.78	150
Beswick	Single Stage Piston Regulator	500	0	450	2.4x 0.688	33g (Al) 72g (Brass),
Beswick	Two-Stage High Pressure Piston Regulator	3000	0	200	2.4844 x 1.03	108
Beswick	Ultra Miniature 3 Stage High Pressure Regulator	3000	0	30	1.09 x 1.03	76
Aircom	High Pressure RH0	3495	8.7	102	3.23 x 1.51	200 g (Al), 430 g (Brass)
Aircom	High Pressure RH1	6000	60; 145	700; 1798	2.99 x 1.51	200 g (Al), 430 g (Brass)

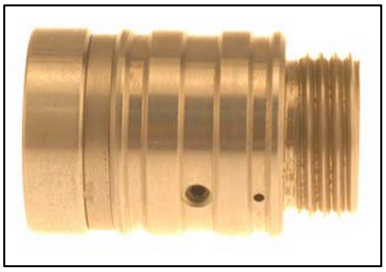

Figure 4: Leland Puncture Device

3.4. Tank Size

Since there are not any COTS refillable gas tanks small enough to fit inside the "3U" CubeSat, a disposable cartridge must be used. The company Leland Gas Technologies was deemed the most appropriate vendor, since they provide a wide range of small cylinder cartridges that can be filled with several gases, including argon, and liquefiable gases, such as carbon dioxide and sulfur hexafluoride. For the purpose of future CGT systems considerations, the tanks were assumed to be refillable when assessing the propellants R-134a and ammonia, in addition to xenon, which also has a high Molar Mass / ISP product and is a commonly used cold gas propellant[5].

For a R-134a CGT system stored at an initial tank pressure of 2750 psi, the minimum tank size required to execute the initial spin-up maneuver and a total reorientation of 360°

[5] Richard Meinhold, Moog Employee.

is 40.75 mL, as founding using the CGT GUI (refer to section 4). Adding a 15% margin to the total reorientation requirement, the new minimum tank size was calculated to be 46 mL. Since the cylinder can extend back towards the main propulsion nozzle but is more constricted on its sides, the diameter of the cylinder was sought to be minimized. Therefore, the chosen propellant tank for R-134a was chosen to be Leland part number 85204Z, which corresponds to a 49 mL tank of diameter 1.125 in. and length 5.50 in. Based on the CGT GUI analysis, this tank size, in conjunction with the rest of the CGT system specifications, should enable a total reorientation of 447°.

If a Xenon CGT system is used, the tank size should be at least 62 mL. To reduce the length such that that cylinder can fit within the spacecraft, the most appropriate gas cartridge was selected to be Leland part number 52053N2, corresponding to a 74 mL tank of diameter 1.50 in. and length 4.50 in.. This xenon-filled cartridge would enable a total reorientation of 540°.

For the candidate argon CGT system, the only prefilled disposable cartridge that Leland Gas Technologies has in stock is 98 mL, which, although fairly large, fits within the spacecraft and provides over 360° of total reorientation (yet under the 15% margin): 374°, as illustrated in Figure 14. The 98 mL tank has a 1.57 in. length and 5.27 in. diameter.

In a similar approach, for a carbon dioxide CGT system, the minimum tank size was calculated to be capable of holding 27.5 g of carbon dioxide. The next disposable cartridge holding above 27.5 g of carbon dioxide that both fit the inlet size of the Leland N-10 regulator (either 3/8”-20 or 5/8”-20) was found to be Leland part number 86121Z, corresponding to 38.0 g of carbon dioxide with tank diameter 1.18” and length 4.65 in. In fact, this length is less than that of the available 29 g disposable cylinder. The 38.0 g tank should theoretically enable a total reorientation of 589°, as illustrated in Figure 13.

If ammonia could be used as the propellant, the minimum tank size required to achieve the required total reorientation with a 15% margin was calculated to be 17.2 g. Since the densities of ammonia and carbon dioxide at 25°C are 602.76 kg/m^3 and 685.5 kg/m^3, respectively, this mass corresponds to 19.6 g of carbon dioxide. Therefore, the tank for an ammonia CGT system would be Leland part number 84201Z, corresponding to 20.0 g of carbon dioxide with a tank diameter 1.00 in. and length 4.05 in.

3.5. Isolation Valve

An isolation valve is beneficial to prevent leakage in the months prior to launch, after the CGT system is fully assembled and the propellant storage tank is punctured, and may be required to allow the pressurized vessel onboard the SLS/Orion EM-1. In particular, the isolation valve should be a normally-closed, latching valve, for which power is applied once to permanently change the valve’s state from closed to open. To reduce leakage most effectively, the isolation valve should be placed immediately at the gas cylinder’s exit; however, because the cylinder must be punctured, it must be placed at the regulator’s exit instead.

An isolation valve small enough to fit in the CGT system and capable of supporting the outlet pressure of the NR-10 regulator (87 psi) was found to be the MEMS Isolation Valve (MIV), which can support up to 2750 psi (proof) and is contained in a titanium housing of outer diameter of 25 mm and mass 86 g, as illustrated in Figure 5. The gas inlet hole is sealed with a metal alloy such that when voltage is applied to the heater element, the generated heat melts the plug, and high gas pressure forces the melted metal

into the chip and opens the gas pas, as illustrated in Figure 6. In addition, the slightly larger Moog Solenoid Actuated Latching Isolation Valve (refer to Figure 7), with a mass of 130 g and proof pressure of 4050 psi, is also a candidate isolation valve. Because the isolation valves may not be very effective when placed after the regulator, and will be better understood through testing, they have not been included in the proposed design.

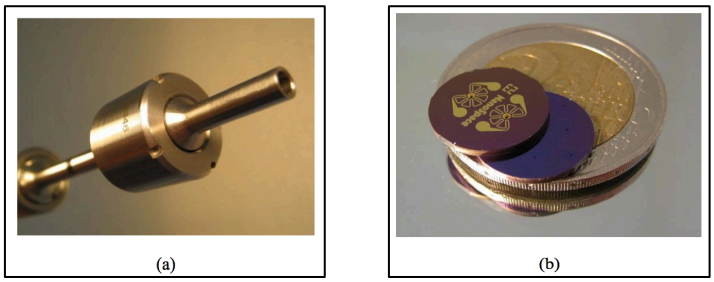

Figure 5: Images of (a) the MEMS Isolation valve housing and (b) separate MIV chips

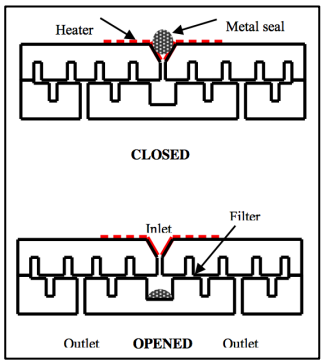

Figure 6: Schematic of (top) the sealed isolation valve and (bottom) the activated valve with free gas path

Figure 7: Moog Solenoid Actuated Latching Isolation Valve

3.6. CMOS Image Processing

The most effective attitude determination solution for the Lunar CubeSat was chosen to be using three CMOS image sensors for several key reasons. First and foremost, sensor options are limited for CubeSats voyaging beyond Low Earth Orbit (LEO), and especially those on lunar trajectories; in particular, GPS, magnetometers, and

horizon detectors loose a great deal of accuracy beyond LEO. Attitude determination is further constrained by the high spin rate of the satellite; star trackers were deemed ineffective due to image blur, and star scanners, which take advantage of spinning spacecraft, were too large and heavy for the Lunar CubeSat. On the other hand, sun sensors were a viable option; the Cubesat Sun Sensor manufactured by SSBV Space 7 Ground Systems was determined to be the optimal sun sensor due to its low mass (~5 g), large field of view (114°), and relatively high accuracy (~0.5°). Nonetheless, the use of sun sensors would only provide one vector in the body frame, the direction of the sun relative to the spacecraft, while at least two are needed in order to relate the body frame to the ECI frame. And, as confirmed by an SSBV employee, the sun sensors cannot distinguish light being reflected off the Earth to obtain a second vector for attitude determination.

CMOS image sensors, on the other hand, would be capable of attaining three vectors in the body frame by imaging the Earth, Moon, and Sun, thus also providing redundancy. Knowing the position of the satellite in the ECI frame through the communications link, the positions of the Earth, Moon, and Sun relative to the spacecraft can be solved for in the ECI frame, and can then be used to determine the rotation matrix relating the spacecraft's body frame to the ECI frame, as depicted in Figure 8. Further, the image blur of the CMOS image sensors can be used in addition to the MEMS L3GD20 gyros as a second estimation of the satellite's spin rate; the shutter speed can be optimized to attain both an effective image for pointing determination and enough blur to determine the angles the spacecraft has rotated during the shutter. Additionally, each CMOS sensor is very small: approximately 26 mm x 20 mm in side-lengths and 16.37 mm in height.

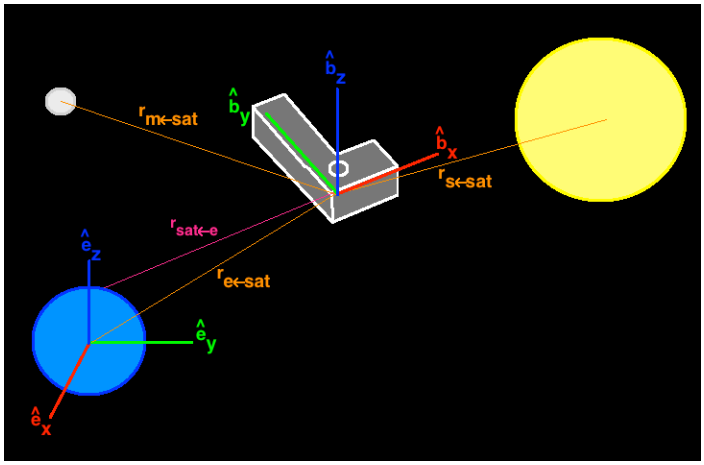

Figure 8: Illustration of vectors used in coordinate transformation between spacecraft's body frame and the ECI frame

In order to determine the vector directions from the spacecraft to the Earth, Moon, and Sun in the body frame, a fisheye to rectilinear conversion will be executed first to achieve an appropriate scale. Next, as suggested by Daniel Hauagge[6], a Hough transform will be implemented to distinguish up to three geometric bodies (i.e., the Earth, Sun,

[6] Hauagge, Daniel. *Graphics and Vision Group*. 455 Rhodes Hall, Cornell University, Ithaca NY 14850.

and/or Moon) within the image, gathering data such as each body's centroid, semi-major axis, and semi-minor axis. Knowing the positions of the CMOS sensors on the satellite as well as their field of view, this data can immediately be used to determine the directional vectors to each body and the angular rates of the spacecraft; the CMOS sensor placed on the rotating side of the spacecraft will calculate the angular rate vector in the image plane, while the two CMOS sensors placed on the top and bottom of the rotating spacecraft will calculate the out-of-plane angular rate vector, as depicted in Figure 9.

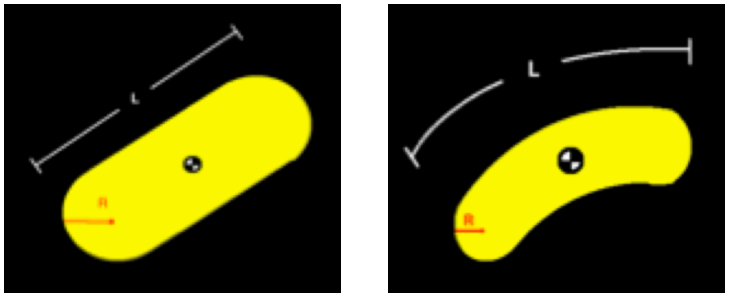

Figure 9: Predicted image blur using side (left) and top/bottom (right) CMOS image sensors

3.7. CMOS Hardware

The selection of a CMOS image sensor for attitude determination on the Lunar CubeSat depends primarily on physical size, pixel array size, exposure time, image control capabilities, and flight experience. Shown in Figure 10, the OV7720 CameraChip™ was found to be the most appropriate CMOS sensor according to these key parameters. First, the sensor is very small relative to other CMOS sensors, with a sensor size of merely 5.345 mm x 5.265 mm and a complete board size of 11.43 mm x 11.43 mm. Next, the OV7720 has a pixel array size of 640 x 480, which is the same as the array size of the ESL CubeSense system, a COTS attitude sensor that uses CMOS sensors to determine sun and nadir directions, and similar to that of the IMEC Fuga 15d (512 x 512), which is a commonly used CMOS sensor for attitude determination[7]. The CubeSense system and Fuga 15d were omitted from the design due to excessive size and limited available information, respectively. The exposure time, also known as "shutter speed", of the OV7720 can be set to a minimum of 8 ms, which, corresponding to a rotation angle of 2.75° when the spin rate of the spacecraft is 6 rad/s, was deemed small enough to avoid excessive image blur. Additionally, the OV7720 CameraChip™ has many automatic image control functions, including automatic exposure control, gain control, white balance, band filter, and black-level calibration, which will all help adjust sensing to the varying lighting conditions of the Earth, Moon, and Sun. Further, the sensor has flight experience on Achen University's COMPASS-1, which launched in April of 2008. Finally, the OV7720 is excellent for image processing; it is commonly used as a high-performance security camera solution incorporating face detection[8], and was claimed to be an optimal CMOS image sensor for microspacecraft image processing

[7] Meller, David. "Digital CMOS Cameras for Attitude Determination". *University of Washington*. 01 July 2000. Web. 09 Apr. 2014.

[8] OV7720 CameraChip™ Datasheet

according to *Camera Design For Pico and Nano Satellite Applications*[9]. The complete specifications of the OV7720 CameraChip™ are provided in Table 4.

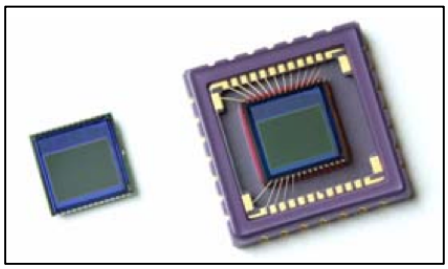

Figure 10: OV7720 Image Sensor (left) and Complete Board (right)

Table 4: OV7720 CameraChip™ Specifications

Array Size	640 x 480
Power Supply (V)	3.0-3.6 (analog), 1.8 ± 10% (digital core), 1.7-3.3 (I/O)
Power Requirements	120 mW (active), <20 µA (standby)
Image Area (µm^2)	3984 x 2952
S/N ratio (dB)	50
Output Format	8-bit YUV/RGB/raw data
Dynamic Range (dB)	60
Pixel Size (µm^2)	6.0 x 6.0
Dark Current (40 mV/s)	40
Scan Mode	Progressive
Temperature Range (°C)	-20 - 70
Package Dimensions (mm^2)	5.345 x 5.265 (CSP2), 11.43 x 11.43 (CLCC)

In order to localize computation associated with image processing algorithms, a TI MSP430 MCU will be used for each OV7720 image sensor. The 10 data output channels of the OV7720 will be connected to the MSP320's digital GPIO pins, and the serial camera control bus (SCCB) will be accessed through the sensor's SDA data and SCL clock pins via I2C connection.

To capture all of space, three OV7720 sensors will be required: one on a rotating face of the spin-stabilized spacecraft, and two others on the top and bottom, as illustrated in Figure 11. They should be placed as close to the spacecraft's center of mass as possible in order to reduce excessive image blur. However, the field of view of each sensor must be greater than 90°; since the OV7720's field of view is only 56°, a fisheye lens is required for each sensor. Some of the smallest COTS fisheye lenses can be mounted to a CMOS camera module using an M12x0.5 lens mount, also known as an S-Mount, which can be purchased through Universe Optics. After speaking with an Edmund Optics professional, the Edmund Optics 110° S-Mount Micro Lens was chosen as the most suitable fisheye lens for the CMOS sensor that will ensure full space coverage, as illustrated in Figure 12. Finally, Edmund Optics Neutral Density Filter Film will be used

[9] Gulzar, Kashif. "Camera Design for Pico and Nano Satellite Applications". *Luleå University of Technology*. 01 Mar. 2010. Web. 10 Apr. 2014.

to appropriately filter the intense light of the Sun; the exact transmissibility of the neutral density filter film will be determined through testing.

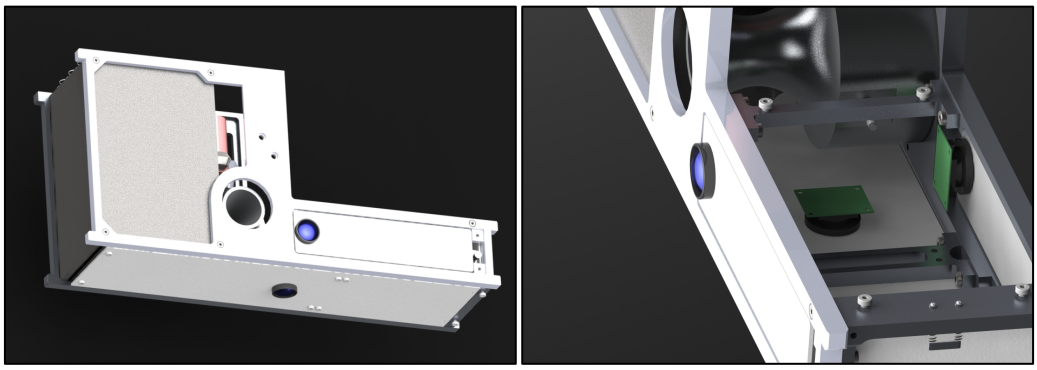

Figure 11: Approximate Locations of Three CMOS Image Sensors

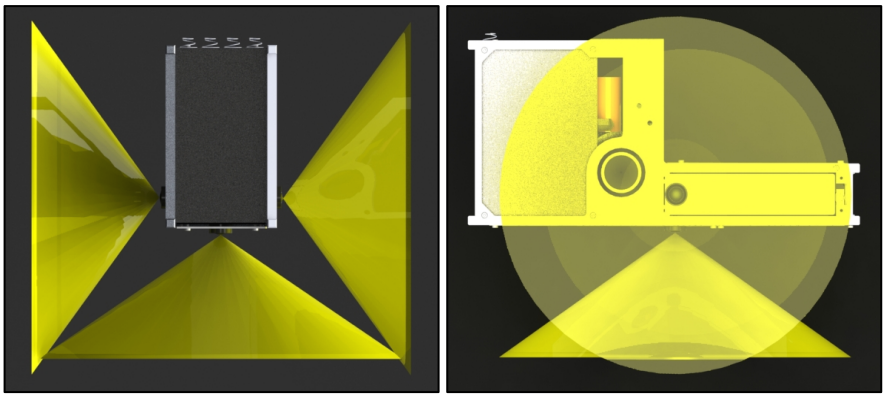

Figure 12: Field of View of CMOS Image Sensors using Edmund Optics 110° S-Mount Micro Lens

4. Analysis

In order to analyze the performance of the CGT system, a MATLAB GUI was developed, as illustrated in Figure 13 and Figure 14. The "Enter" button can be clicked to run a CGT simulation after the following steps have been completed: selecting a gas or liquefiable gas from the dropdown menu (or by manually entering the propellant's molar mass and ISP) and entering the initial pressure and volume of the disposable gas cartridge or the initial mass of the liquefiable gas, the average temperature of the CGT system, initial thrust of the cold gas micro-thruster, pulse time or angle through which to command the thruster "on", satellite spin and mass properties, and finally the desired precision of the spin-up maneuver. When the simulation finishes, the total reorientation angle of the satellite, as well as the precision achievable at each pulse (i.e., half the change in the reorientation angle), is plotted as a function of pulse number, and additional results shown in the bottom-right panel of the GUI are displayed. The constrain that ends the simulation can be selected as either a final propellant mass, which is set to 0 by default to indicate that all propellant should be used, or a final reorientation angle.

The simulation ran by the GUI, written within the `enterBtn` callback function of *cgtGUI.m*, begins by calculating the amount of propellant required for the initial spin-up maneuver. Since the satellite will separate from the SLS/Orion EM-1 vehicle with

negligible spin, the first CGT pulse will set the spacecraft's spin-up angular momentum, assuming that the torque applied by the CGT system is in the same direction—or, in other words, that the spacecraft does not significantly begin to settle into its stable spin about the maximum-moment-of-inertia axis during the initial pulse. Therefore, for each additional pulse, the reorientation of the satellite's angular momentum vector becomes the following:

$$\Delta\phi_{pulse} = \frac{rI_{pulse}}{H_0} = \frac{r\left(F_{thrust}\Delta t_{pulse}\right)}{r\left(F_{thrust}\Delta t_{spin-up}\right)} = \frac{\Delta t_{pulse}}{\Delta t_{spin-up}} \quad \textbf{(Eq. 3)}$$

where $\Delta t_{spin\text{-}up}$ is the initial pulse time required for spin up and Δt_{pulse} are the subsequent pulse time required for reorientation, and $\Delta\phi_{pulse}$ is twice the precision required for spin up (±5°). The spin-up maneuver ends once the satellite reorients by 180°—the worst-case reorientation requirement during spin up resulting from the main propulsion nozzle facing the complete opposite direction than desired for the first maneuver.

In order to minimize the mass required for reorientation, Δt_{pulse} is taken to be the combined response time of the cold gas micro-thruster, which consists of the opening plus closing response time; this pulse is known as the thruster's minimum impulse bit. In turn, $\Delta t_{spin\text{-}up}$ is calculated by simply multiplying Δt_{pulse} by $\Delta\phi_{pulse}$, after which the mass to reorient 180° is calculated.

Next, the simulation proceeds to the main while loop, which includes a function that takes in the pulse force and propellant mass and outputs $\Delta\phi_{pulse}$, or the change in angle of the spacecraft's angular momentum vector, as well as the new propellant mass. $\Delta\phi_{pulse}$ is calculated using the small-angle-approximated reorientation equation (Eq. 2), and the new mass is calculated by the following equation:

$$m_{n+1} = m_n - \dot{m}\Delta t_{pulse} = m_n - \left(\frac{F_n}{ISP \cdot g_0}\right)\Delta t_{pulse} \quad \textbf{(Eq. 4)}$$

where m_n and F_n refers to the propellant mass and thrust at pulse n and m_{n+1} to the new propellant mass. After a pulse is fired, the simulation moves on to calculate the thrust of the next pulse given the new mass. Modeled as linearly proportional to the propellant tank's current pressure, the next thrust was calculated as follows assuming the propellant is an ideal gas:

$$F_n = \left(\frac{F_0}{P_{F_0}}\right)P_n = \left(\frac{F_0}{P_{F_0}}\right)\left(\frac{m_n RT}{MM \cdot V}\right) \quad \textbf{(Eq. 5)}$$

where F_n is the thrust of the next pulse, P_n is the current pressure in the tank, F_0 is the original thrust of the thruster, and P_{F0} is the operating pressure of the thruster (i.e., the pressure at which F_0 was recorded). If a liquid propellant is used, its estimated vapor pressure curve is used to obtain the tank pressure at the given temperature. For both gas or liquefiable gas propellant, the regulator is also modeled into the simulator; if the tank pressure at pulse n is greater than the regulated pressure, then the regulated pressure is simply used for P_n.

In order to increase the accuracy of the simulation, the change in the spacecraft's spin-axis moment of inertia is taken into consideration by assuming that it varies linearly from its value when the main propulsion tank is full (i.e., at the start of the mission) to its value when the tank is completely empty (i.e. at the end of the mission) as a function of CGT pulse number. In other words, each CGT pulse is associated with an equally spaced change in moment of inertia. To implement this as a user of the CGT GUI, the full and empty spin-axis moments of inertia are entered in the bottom-left in the panel, a simulation is ran to obtain the total number of pulses, this value is entered into the "# Pulses" text box in the bottom-left panel, and finally the "Enter" button is clicked again to attain more accurate simulation results through linearly interpolating the spin-axis moment of inertia as a function of pulse number. The two final analysis results for the CO_2- and Ar-based CGT systems are provided in the tables that follow.

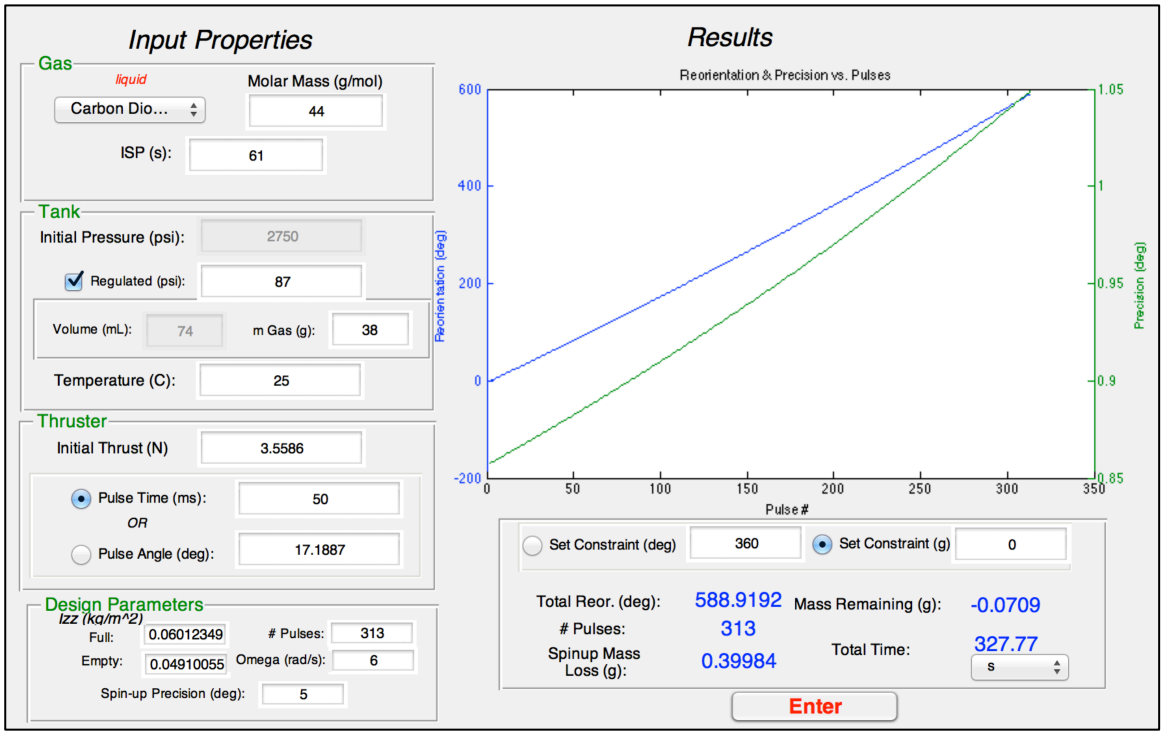

Figure 13: Simulation Results for a CO_2-Based CGT System

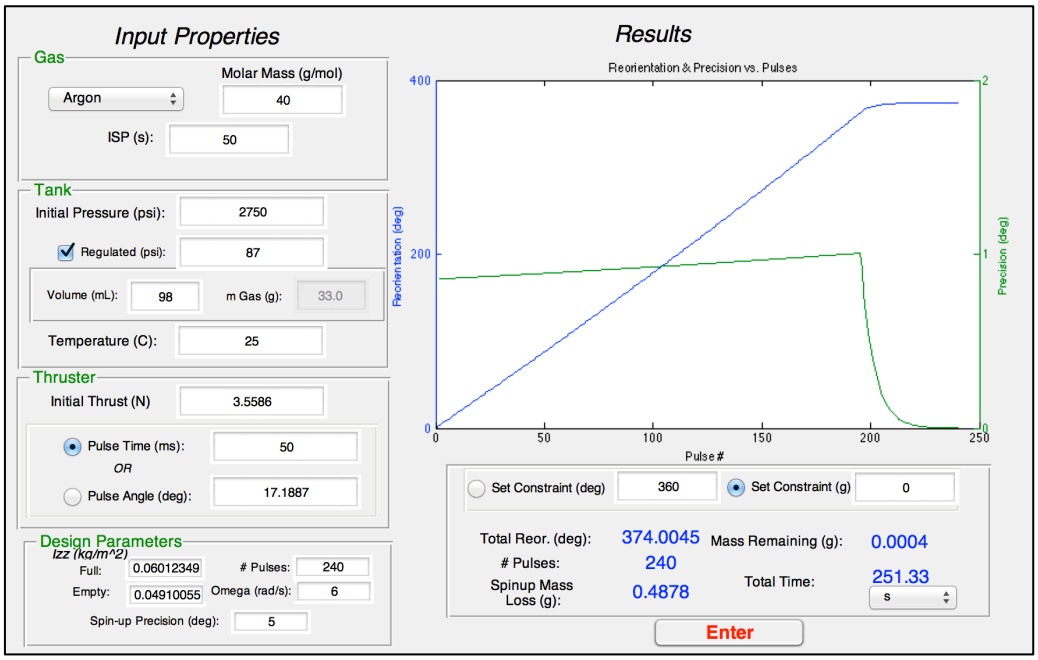

Figure 14: Simulation Results for an Ar-Based CGT System

5. Results

A representation of the final cold gas thruster assembly is provided below in Figure 15 for the CO_2-based CGT system, with alternative specifics for the Ar-based CGT system given in parenthesis:

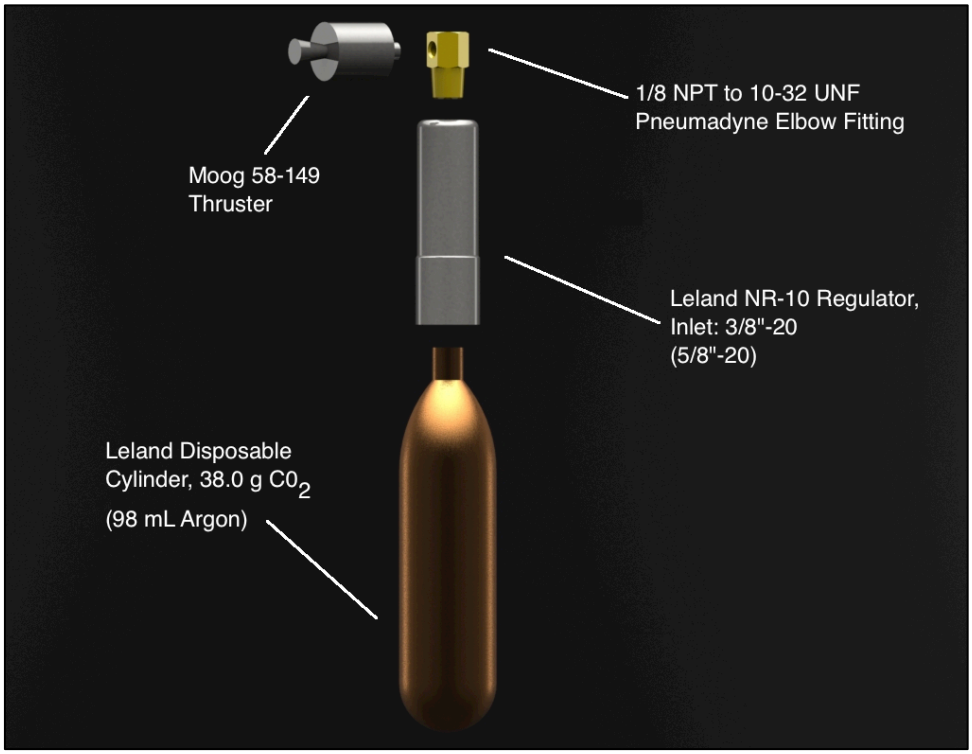

Figure 15: CO_2-Based CGT System, with argon components in parentheses

Next, candidate layouts of the candidate CO_2- and Ar-based CGT systems within the spacecraft are provided in Figure 16 and Figure 17, respectively. These layouts also include the three CMOS cameras. Both the CMOS cameras and the thruster protrude 6 mm from the outer surface of the spacecraft, which is acceptable according to the 6U sizing requirements, in order to maximize the space available for the CGT system. Additionally, the CGT system is place as close to the inner wall of the satellite as possible to leave more room for additional hardware, such as the avionics boards.

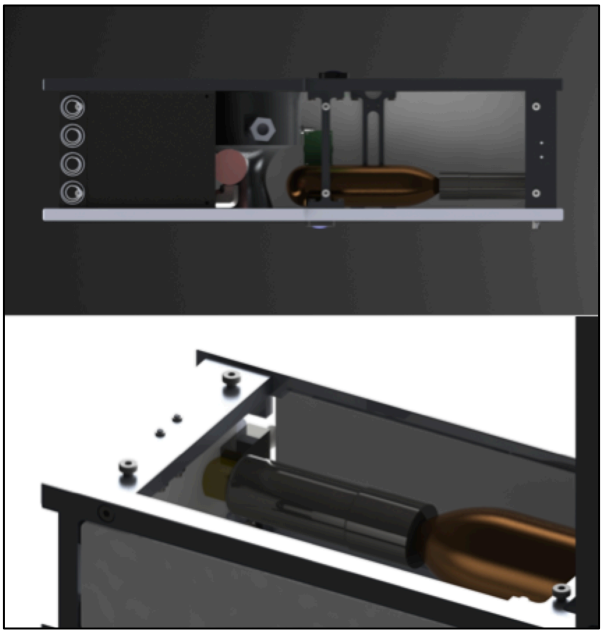

Figure 16: CO_2-Based CGT System

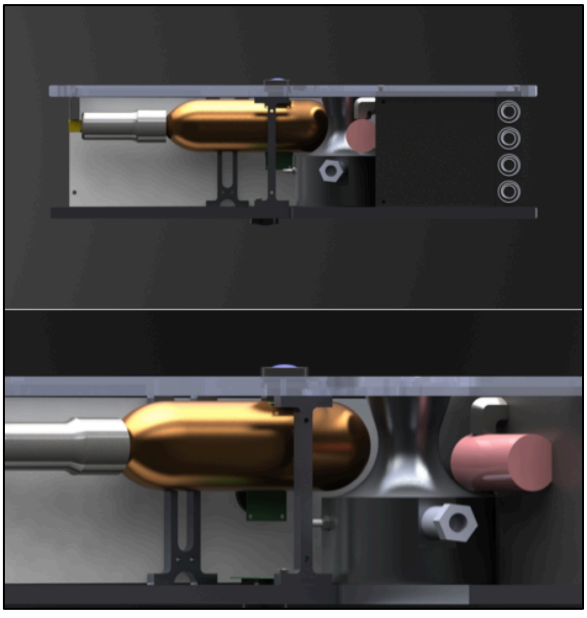

Figure 17: Ar-Based CGT System. Note: thruster cannot protrude 6 mm due to tank's large width

As illustrated by the SolidWorks models, using argon as the propellant creates the need for a much larger CGT system than the carbon dioxide system. In fact, the large tank size completely prevents the addition of an isolation valve. Thus, although using a pure gas propellant is more simple and reliable, carbon dioxide was chosen as the propellant choice for the Lunar CubeSat CGT system.

Last, the entire CMOS attitude determination module is shown in Figure 18, with approximate dimensions of 26 mm x 20 mm in side-lengths and 16.5 mm in height.

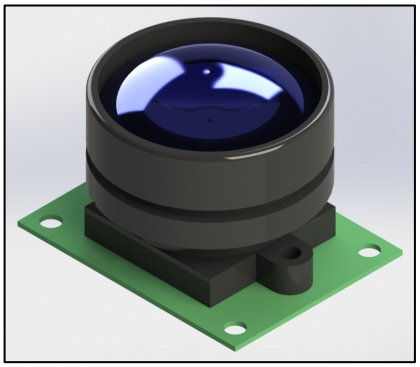

Figure 18: CMOS Attitude Determination Module

6. Future Work

As stated earlier in the report, liquid propellants with lower vapor pressures than carbon dioxide should be considered for the CGT design in order to eliminate the need for a regulator, which could reduce the system's size and leakage. More importantly, if a liquid propellant is used, the layout of the CGT should be reversed such that the propellant tank's top seal is pointed towards the center of the spacecraft. This will most likely be necessary since the satellite will be spinning, meaning that all liquid will move outward; in the current CGT design, then, liquid may flow through the system, which could both damage the regulator and thruster and waste propellant. An example of what the improved CGT should look like is provided in Figure 19. Next, analysis regarding the change in pressure and temperature of the propellant tank after each pulse as a function of time should be conducted, which can be done by using the ideal gas law and the rate of evaporation simultaneously. This analysis will determine the appropriate amount of time required between pulses such that the pressure and temperature of the propellant tank are not too low. Additionally, to further reduce leakage, either the MEMS Isolation Valve or the Moog Solenoid Actuated Latching Isolation Valve should be incorporated into the system for testing. Last, disposable cylinders that can be filled with either R-134a or xenon, or other high molar mass / ISP product gases such as Freon 12, should be further investigated.

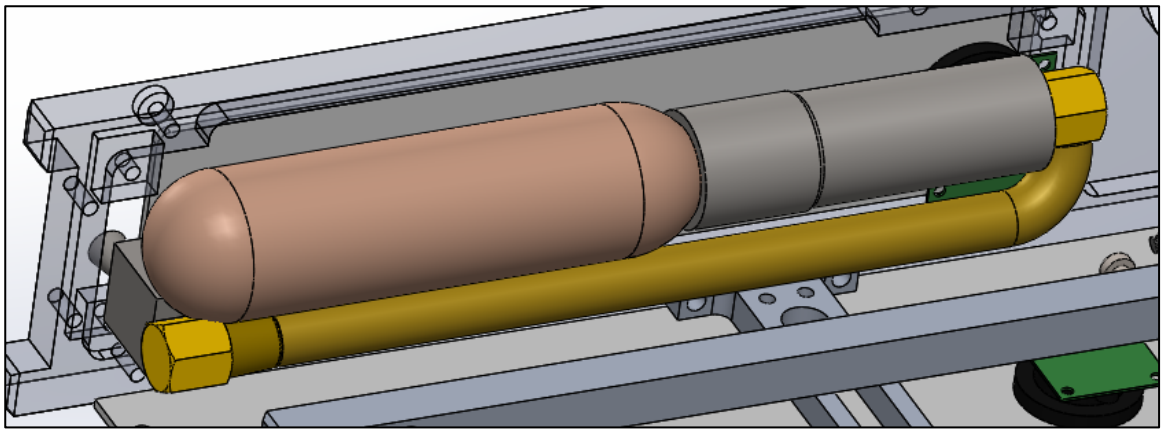

Figure 19: Example of improved of liquid CGT System model, with the propellant tank pointed in the reverse direction to prevent liquid from flowing through the system.

Several test procedures should be conducted to ensure that the CGT analysis is being conducted properly, and also to obtain a better understanding of the system. First and foremost, upon ordering and assembling the Leland 38.0 g 86121Z disposable cylinder and NR-10 regulator, the outlet pressure of the regulator should be obtained to ensure that it is 87 psi, and to get its exact value; in place of the Moog thruster, another solenoid valve should be used. Next, this assembly should be left in tact for a long period of time in order to measure the leakage rate. Another assembly, with the addition of the isolation valve, should also be tested for leakage in order to determine the effectiveness of the isolation valve, and whether or not it is worth the added complexity.

In addition, the temperature and pressure of the tank after a pulse should be measured in order to validate analytical results if possible. Pressure could be measured by using a Leland puncture device in place of a regulator, with a pressure sensor on the outlet of the puncture device connected to a solenoid valve.

Last, the entire system, composed of the carbon dioxide propellant and its storage tank, NR-10 regulator, threaded fittings and most likely tubing, and the Moog 58-112 thruster, should be tested. First, the actual mass flow rate, ISP, and thrust of the system should be measured. In addition, using the same pulse time as the simulations, the CGT system should be fired starting with a full tank of propellant until no more propellant remains, measuring the thrust with each pulse, in order to compare the experimental results with the CGT GUI analysis.

For the CMOS attitude determination sensor, the first test should be simply assembling the camera and capturing an image. After this is complete, the primary task would be to figure out the optimal transmissibility percentage of the Edmond Optics neutral density filters by taking images of the Sun and full Moon while sampling different films. Next, the capability and effectiveness of identifying a body by either its color or light intensity should be tested by again imaging the Sun and full Moon. Further, although the image quality would most likely be significantly better, images found online of the Earth, Moon, and/or Sun in the same frame may be helpful to run through the initial body-identification algorithm. Finally, the Hough Transform algorithm should be used when imaging the Sun and full Moon to determine position and angular velocity vectors in the body frame. Non-full Moons should be tested as well to test the algorithm's robustness.

7. Conclusion

Through determining and beginning design of the Lunar CubeSat Project's ACS actuators and sensors, candidate models of the CGT system and CMOS attitude determination image sensors have been developed. The components of the CGT system involve a Leland 38.0 g carbon dioxide disposable cylinder, Leland NR-10 regulator, Pneumadyne Elbow Fitting (1/8 NPT male to 10-32 UNF female), and Moog 58-122 cold gas micro-thruster. As opposed to Argon, which is excessive in size and thus prevents system modularity (which may be required for additions such as the isolation valve), carbon dioxide enables greater reorientation capabilities using a smaller tank, and was therefore chosen as the system's propellant. The characteristics of the CGT system, including propellant capabilities, gas tank pressure and size, and micro-thruster force, had been analyzed adequately through frequent use and refinement of the CGT MATLAB GUI. However, as explained in the "Future Work" section of this report, much testing will be required before the system is fully understood and a final design can be made.

As for the CMOS attitude sensor, the OV7720 CameraChip™ had been selected primarily due to its small size, effective pixel array size and exposure time, flight experience, and its current involvement with image processing. Although the hardware has been selected for the CMOS attitude sensor, extensive testing (as also explained under the "Future Work" section) will be required to (a) determine the optimal neutral density filter transmissibility, (b) the effectiveness of the Hough Transform image processing algorithm, and (c) the accuracy of the entire system in attaining valid position and angular velocity vectors in the body frame to, in conjunction with the MEMS L3GD20 gyros, attain the full attitude solution of the spacecraft.

8. References

8.1. Cold Gas Thrusters

Anis, Assad (2012). "Cold Gas Propulsion System – An Ideal Choice for Remote Sensing Small Satellites". *NED University of Engineering and Technology*. Web. 07 Mar. 2014.

Berkovitz, D. S., "System Characterization and Online Mass Property Identification of the SPHERES Formation Flight Testbed," S.M. Thesis, Department of Aeronautics and Astronautics, Massachusetts Institute of Technology, Cambridge, MA, 2008.

Burges, J.D., Hall, M.J., Lightsey, E.G."Evaluation of a Dual-Fluid Cold-Gas Thruster Concept.International Journal of Mechanical and Aerospace Engineering. 01 June 2012. Web. 16 May 2014.

Makled, A. E., Al-Sanabawy, M. A., Bakr, M.A. "Theoretical and Experimental Evaluation of Cold Gas System Components". *Aerospace Sciences 7 Aviation Technology*. 26 May 2009. Web. 15 Mar. 2014.

Mauthe, Stephen; Pranajaya, Freddy; Zee, Robert E. "The Design and Test of a compact Propulsion System for CanX Nanosatellite Formation Flying". 05 June 2005. Web. 30 Apr. 2014.

Mueller, Juergen (1997). "Thruster Options for Microspacecraft: A Review and Evaluation of Existing Hardware and Emerging Technologies." *Jet Propulsion Laboratory*. Web. 14 Mar. 2014.

Mueller, Juergen; Ziemer, John; Hofer, Richard; Wirz, Richard; O'Donnell, Timothy. "Survey of Micro-Thrust Propulsion Operations for Microspacecraft and Formation Flying Missions". *Jet Propulsion Laboratory*. 09 Apr. 2008. Web. 07 Mar. 2014.

Nguyen, Hugo; Köhler, Johan; and Stenmark, Lars. "The Merits of Cold Gas Micropropulsion In State-Of-The-Art Space Missions". *The Ångström Space Technology* Centre. 02 February 2007. Web.

8.2. R-134a Propellant

Pahl, Ryan A., Tutza, Christopher P. "Design, Test, and Validation of a Refrigerant-Based Cold-Gas Propulsion System for Small Satellites". *Missouri University of and Technology*. 09 Aug. 2010. Web. 12 Apr. 2014.

Seubert, Carl R., Miller, Shawn W., Siebert, Joseph R. , Stweart, Abbie M., Pernicka, Henry J. "Feasibility of Developing a Refrigerant-Based Propulsion System for Small Spacecraft". *University of Missouri-Rolla*. 04 March. 2007. Web. 12 Apr. 2014.

8.3. MEMS Isolation Valve

Bejhed, J., Jonsson, K., Grönland, T-A., and Rangsten, P. "Advanced Flow Control Devices based on MEMS Technology for Electric Propulsion". 06 October 2013. Web. 16 May. 2014.

Rangsten, Pelle; Johansson, Håkan; Bendixen, Maria; Jonsson, Kerstin; Bejhed, Johan; and Gröland, Tor-Arne. "MEMS Micropropulsion Components for Small Spacecraft". *NanoSpace AB*. 02 Oct. 2011. Web. 16 May. 2014.

8.4. CMOS Image Sensor

Gulzar, Kashif. "Camera Design for Pico and Nano Satellite Applications". *Luleå University of Technology*. 01 Mar. 2010. Web. 10 Apr. 2014.

Meller, David. "Digital CMOS Cameras for Attitude Determination". *University of Washington*. 01 July 2000. Web. 09 Apr. 2014.

Ogiers, W., Uwaerts, D., Dierickx, B., Scheffer, D., Meynants, G., and Truzzi, C. "Compact CMOS Vision Systems for Space Use". *IMEC*. Web. 10 Apr. 2014.

8.5. General

LCP-ADCNS-002: ADCNS Requirements

Smith, Cam. "Systems Design Overview of the EPRP Spacecraft". *Cornell University*. 23 Feb. 2014.

"Small Spacecraft Technology State of the Art". *National Aeronautics and Space Administration*. Feb. 2014. Web. 27 Feb. 2014.

Zeledon, Rodrigo A., and Peck, Mason A (2013). "Attitude Dynamics and Control of a 3U CubeSat with Electrolysis Propulsion. *Cornell University*.

9. Appendix

Appendix A: Moog 58-149 Cold Gas Micro-Thruster

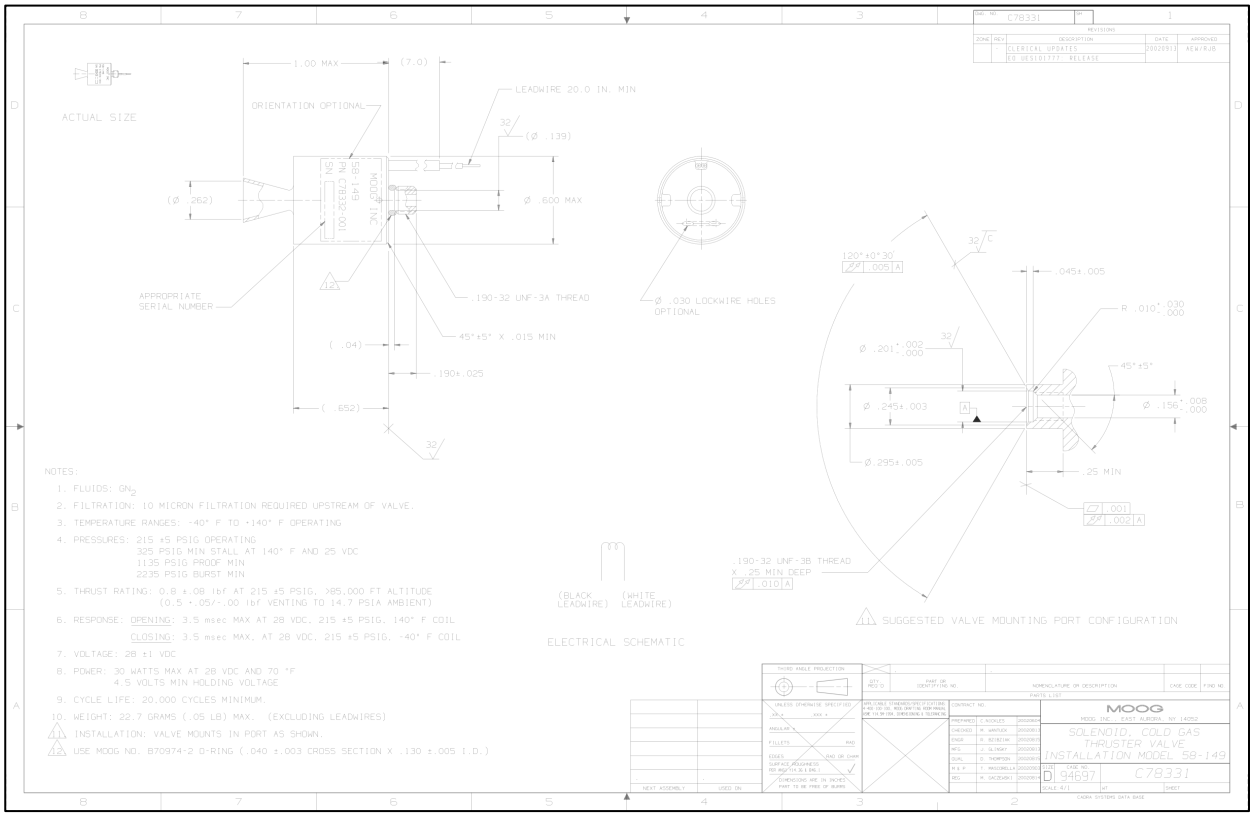

Appendix B: Leland NR-10-50049 Regulator

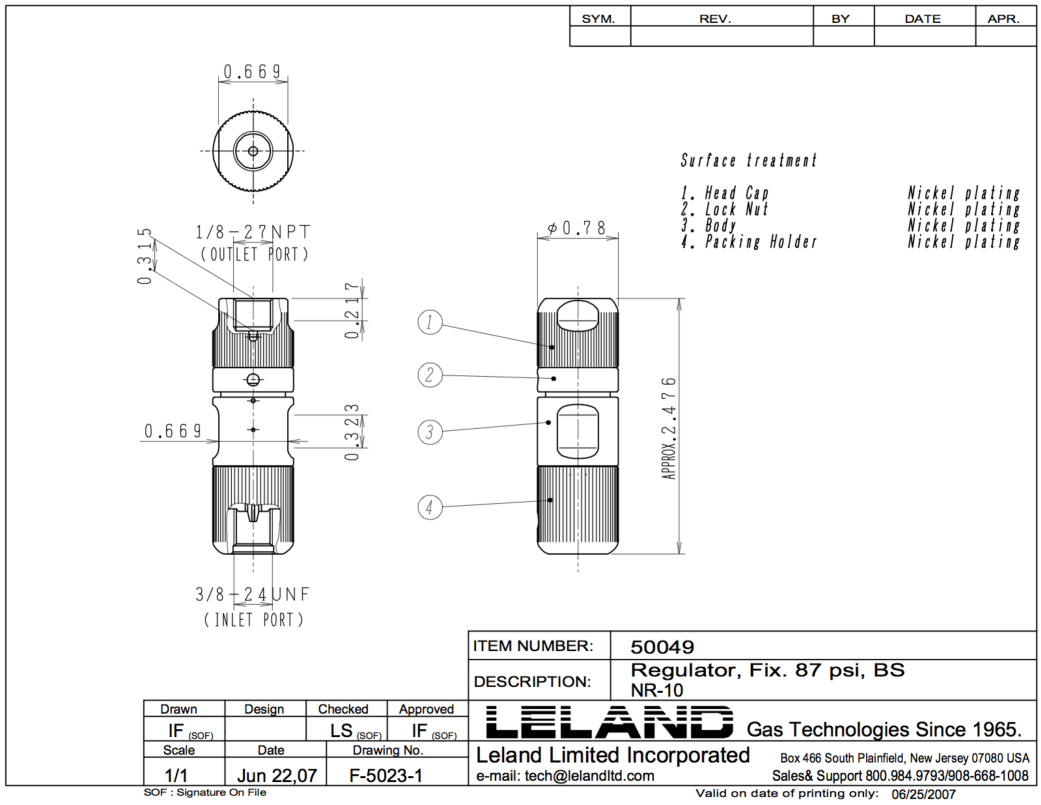

Appendix C: Edmund Optics 110° S-Mount Micro Lens